Nucleation and Growth of Succinic Acid in a Batch Cooling Crystallizer

Yanfeng Qiu and Åke C. Rasmuson
Dept. of Chemical Engineering, Royal Institute of Technology, S-100 44 Stockholm, Sweden

A method to evaluate nucleation and crystal growth rates from batch cooling crystallization experiments is presented. Solute concentration and suspension temperature are recorded during the experiment and the product crystal size distribution is analyzed. The crystal growth and nucleation rates at any instant are calculated by solving the population balance equation using the method of characteristics, together with the mass balance equation. Based on a set of different cooling crystallization experiments, kinetics for succinic acid are determined. Applying these kinetics in process simulation allows for a reasonably accurate prediction of the product weight mean size.

Introduction

Modeling and design of batch crystallizers suffer from lack of adequate kinetic data for crystal growth and in particular for nucleation. Nucleation rates are sensitive to the specific design of the crystallizer and to process conditions. The classical MSMPR (mixed suspension mixed product removal) technique (Randolph and Larson, 1971) has been used extensively to determine nucleation and growth rates in laboratory experiments. While the evaluation is very simple theoretically, it is experimentally difficult to fulfill the assumptions and its method is time-consuming. The supersaturation level in a continuous crystallizer is very low for fast-growing systems so that the measurement of kinetics at a high supersaturation level becomes difficult. There is a growing interest in nonstationary experiments since they are capable of providing more information from one experiment and in certain aspects are easier to perform.

Seeded batch isothermal experiments (Tanimoto et al., 1964; Bujac and Mullin, 1969; Qiu and Rasmuson, 1990) have been proved to be an efficient way of obtaining the relation between the crystal growth rate and supersaturation, when nucleation is suppressed. The decay in supersaturation is measured and through a mass balance related to the growth of seed crystals. To extract information concerning nucleation, size distributions have to be determined. Misra and White (1971) and Ness and White (1976) used population balance equation to obtain both the nucleation rate and the crystal growth rate from the measurements of crystal size distributions during the experiment. Tavare and Garside (1986) improved the accuracy of this method by Laplace transformation of the population balance equation. The growth rate is assumed to be size-independent.

Bransom and Dunning (1949) calculated kinetic parameters from the product crystal size distribution. Omran and King (1974) made a similar analysis for ice crystallization and used the thermal response to characterize the process. Verigin et al. (1979) estimated nucleation and growth rates from the final crystal size distribution and the concentration measurements during a batch cooling experiment. The population balance equation and the mass balance equation were solved using the method of finite differences. Kinetic parameters for both nucleation and crystal growth are determined by the method of successive approximations. Unfortunately, details of the method are not given. In a similar approach by Nyvlt (1989), the size distribution is approximated by a specific function. Marchal et al. (1988) designed a set of semibatch cooling crystallization experiments to evaluate 11 parameters for nucleation, growth and agglomeration by a stepwise nonlinear optimization. Experimental data used comprise recordings of solute concentration and particle size distribution during the experiments. Witowski et al. (1990) include recordings of concentration and particle light obscuration of a batch experiment, in evaluating four parameters of nucleation and growth by nonlinear optimization.

Previous crystallization studies of succinic acid focus only on the crystal growth rate (Mullin and Whiting, 1980; Davey et al., 1982; Qiu and Rasmuson, 1990). In this study, seeded

Correspondence concerning this article should be addressed to Å. C. Rasmuson.

batch cooling crystallization experiments have been performed to obtain both nucleation rates and crystal growth rates simultaneously. The solute concentration and the temperature of the suspension are measured during the experiment, and the final product crystal size distribution is analyzed by sieving. The population balance equation is solved by the method of characteristics to extract kinetic parameters of nucleation and crystal growth.

Mathematical Model

Consider a well-mixed batch cooling crystallizer in which crystal breakage, agglomeration and crystal growth rate dispersion are negligible. Assume that evaporation of the solvent may be neglected, that all crystals have the same shape, and that nuclei are born at a negligible size. For this case, the population balance equation can be written as (Randolph and Larson, 1971):

$$\frac{\partial n}{\partial t}+\frac{\partial (Gn)}{\partial L}=0 \tag{1}$$

with the initial condition

$$n(0,\ L)=n_0 \tag{2}$$

and the boundary condition

$$n(t,\ 0)=B/G(\Delta c,\ 0) \tag{3}$$

n_0 denotes the population density distribution of the seeds. The crystal growth rate G and nucleation rate B may be functions of supersaturation, crystal size, magma density, temperature, and degree of agitation. Equation 1 is a first-order partial differential equation. If the crystal growth rate G can be expressed as a product of a function of supersaturation and a function of crystal size:

$$G(\Delta c,\ L)=f(\Delta c)g(L) \tag{4}$$

we may derive at

$$\frac{\partial n}{\partial t}+G\frac{\partial n}{\partial L}=-f(\Delta c)\ n\frac{\partial g(L)}{\partial L} \tag{5}$$

Equation (5) is a first-order quasilinear equation. The solution is a surface $n=n(t,\ L)$ and can be represented by a family of characteristic curves (John, 1978). Along each characteristic curve the relation

$$dt=\frac{dL}{G}=\frac{dn}{-f(\Delta c)\ n\dfrac{\partial g(L)}{\partial L}} \tag{6}$$

holds. By integration of Eq. 6, such a curve can be expressed as:

$$n(t_2,\ L_2)=n(t_1,\ L_1)\ g(L_1)/g(L_2) \tag{7}$$

and

$$L_2=L_1+\int_{t_1}^{t_2} G\ dt \tag{8}$$

For the crystals which are born at time θ, the size and the population density at time t can be calculated from Eqs. 3, 4, 7 and 8 as:

$$n\ (t,\ L)=\frac{B(\theta)}{G(\Delta c(\theta),\ L)} \tag{9}$$

and

$$L=\int_{\theta}^{t} G\ dt \tag{10}$$

The total mass of solute substance is constant, but the solute concentration in solution decreases during the process as related to the deposition of the solid material:

$$c+W=c_0+W_0=\text{const.} \tag{11}$$

Differentiating Eq. 11 results in

$$-\frac{dc}{dt}=3k_v\rho\int_0^{\infty} L^2G(\Delta c,\ L)\ n\ dL \tag{12}$$

and by insertion of Eq. 4 the growth rate function $f(\Delta c)$ may be obtained as:

$$f(\Delta c)=-\frac{dc}{dt}\Big/\left[3k_v\rho\int_0^{\infty} L^2g(L)\ n\ dL\right] \tag{13}$$

Nucleation rates may be calculated from Eq. 3 or 9.

Numerical Solution

Consider evaluation of nucleation and growth kinetics from a batch cooling crystallization experiment. An initially supersaturated or saturated solution is seeded by a known amount of seeds. The suspension is gradually cooled along a desired temperature profile or by natural cooling. Temperature and concentration are carefully recorded during the process, and after completion the size distribution of the product is determined. The solubility-temperature relation is assumed to be known. If the crystal growth rate is size-dependent, the size dependency function $g(L)$ can be determined in a separate experiment, in which only the crystal size distributions at two different times of a batch experiment are determined (Qiu and Rasmuson, 1989). No measurements on temperature, concentration or supersaturation are needed. In the following, it is assumed that the growth rate function $g(L)$ is known or the growth rate is size-independent.

Adopting the mathematical formulation above the calculation starts from the final state of the process and is performed backward in time. The product crystal size distribution is used as "initial" crystal size distribution. From the population and mass balance equations, the crystal size distribution at any time during the experiment can be calculated by a simple Eulerian stepping technique. Either steps in crystal size or steps in time may be used as independent variables. If the time is

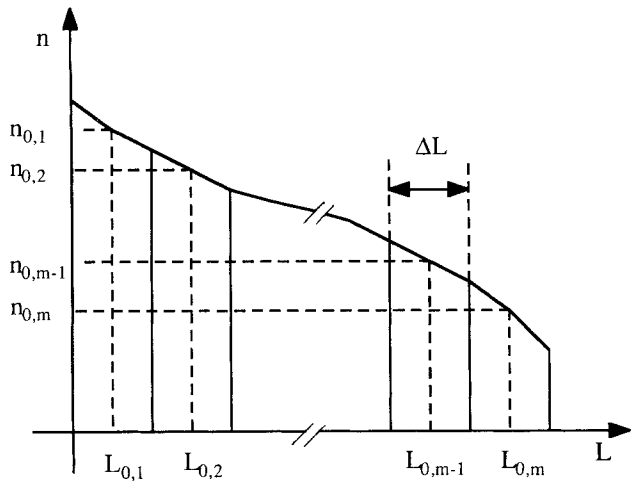

Figure 1. Discretization of the population density function.

chosen (as done by Nyvlt, 1989), an implicit equation must be solved in each step to find the corresponding size changes, while stepping in size makes the corresponding calculation explicit. Furthermore, equal size steps generate a better allocation of the calculation effort. Calculation in terms of equal time steps becomes dominated more by low supersaturation periods. Thus, in our calculations stepping in size is used. The population density distribution of product crystals is divided into m groups, with the average sizes $L_{0,1}$, $L_{0,2}$, ..., $L_{0,m}$ ($L_{0,1} < L_{0,2} \ldots < L_{0,m}$) and population densities $n_{0,1}$, $n_{0,2}$, ... $n_{0,m}$. The first index denotes the step number in the calculation procedure and relates to the actual size of each group in the step. The second index specifies the group in question by relating to the product distribution. If all the size intervals are equal, i.e., $L_{0,i+1} - L_{0,i} = \Delta L$, for $i = 1, 2, \ldots m$, and the crystal size interval ΔL is very small, the numbers of crystals per unit mass of solute in each size interval can be approximated by $\Delta L n_{0,1}$, $\Delta L n_{0,2}$, ... $\Delta L n_{0,m}$, Figure 1. In each step, the population near the abscissa is moved to zero size. If the growth rate is size-independent, the whole distribution moves along simply by horizontal translation. In the case of size-dependent growth, larger particles decrease in size more or less than smaller ones.

By summing up all of the size changes, we obtain the total change in crystal mass corresponding to a change in solute concentration in solution. Using the measured concentration vs. time data, the time step corresponding to the step taken in size may be determined. The growth rate is calculated from the slope of the concentration vs. time curve and the total area of crystals according to Eq. 13. Using the measured temperature curve, the solubility and thus supersaturation generating this growth rate may be calculated. The nucleation rate is obtained from the population density of particles reduced to zero size and the growth rate.

In the case of size-dependent growth, the ΔL translations in one step related to the size as

$$\int_{L_{i-1,j}}^{L_{i,j}} \frac{dL}{g(L)} = \int_{L_{i-1,j+1}}^{L_{i,j+1}} \frac{dL}{g(L)} = \int_{L_{i-1,j+2}}^{L_{i,j+2}} \frac{dL}{g(L)} = \ldots \tag{14}$$

as obtained from Eq. 4 (Baliga, 1970). If ΔL is small, Eq. 14 can be approximated by

$$\frac{L_{i,j+1} - L_{i-1,j+1}}{L_{i,j} - L_{i-1,j}} = \frac{g(L_{i-1,j+1})}{g(L_{i-1,j})} \tag{15}$$

In the ith step, the product crystals having the size $L_{i-1,i}$ move to zero size. The product crystals having sizes larger than $L_{i-1,i}$ decrease according to:

$$L_{i,j} = L_{i-1,j} - L_{i-1,i} \frac{g(L_{i-1,j})}{g(L_{i-1,i})} \quad (j = i,\ i+1,\ i+2,\ \ldots,\ m) \tag{16}$$

The numbers of crystals that have the size $L_{0,i}$ at the end of the experiment are not changed during the calculation:

$$\Delta N_j = \Delta L n_{0,j} \quad (j = 1,\ 2,\ 3,\ \ldots,\ m) \tag{17}$$

In each step, the new size of each population is stored. The mass of total crystals after size reduction is calculated by numerical integration

$$W_i = k_v \rho \sum_{j=i}^{m} L_{i,j}^3 \Delta N_j \tag{18}$$

and concentration of the solute becomes:

$$c_i = c_0 + W_0 - W_i \tag{19}$$

The time t_i can be calculated from the spline function: $c = c(t)$. The supersaturation at that moment is obtained from the spline function: $T = T(t)$ and the solubility function:

$$\Delta c_i = c_i - c^*[T(t_i)] \tag{20}$$

The supersaturation-dependent part of the growth rate function is calculated from Eq. 13, in which the denominator of the righthand side is calculated numerically as:

$$\int_0^\infty L^2 g(L)\, dN = \sum_{j=i}^{m} L_{i,j}^2 g(L_{i,j}) \Delta N_j \tag{21}$$

The nucleation rate is calculated by rearranging Eq. 9:

$$B_i = n_{0,i} f(\Delta c_i)\, g(L_{0,i}) \tag{22}$$

which finishes the calculations of the ith step. The computer program outputs the time, supersaturation, temperature, total mass of crystals, crystal growth rate, and nucleation rate in each step of calculation. When the total mass of crystals becomes smaller than the mass of seeds, the calculation is stopped.

If the crystal growth rate is size-independent, $g(L) = 1$, $G(\Delta c) = f(\Delta c)$, and the crystal growth and nucleation rates can be calculated by the same procedure described above. Instead of using Eqs. 13 and 22, the growth rate may be calculated by taking the ratio of the size step and the corresponding calculated time step and the nucleation rate as the number of crystals reaching zero size divided by the time step. This would correspond to a discretization of Eqs. 13 and 22, and should produce results very close to those of the technique used, if the steps taken are small enough. In checking this, discrepancies are found to be negligible for the step length applied. When the steps are large, Eqs. 13 and 22 give better results than using discretization.

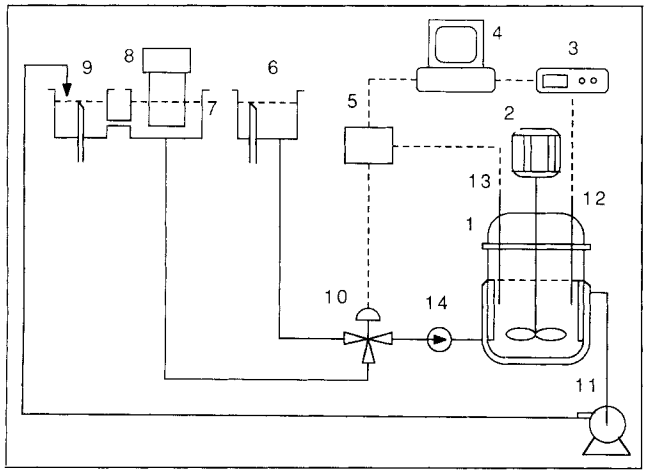

Figure 2. Experimental apparatus.

1. crystallizer
2. motor
3. data acquisition and control unit
4. computer
5. controller
6. cold water tank
7. hot water
8. heater
9. overflow tank
10. valve
11. pump
12, 13. thermometer

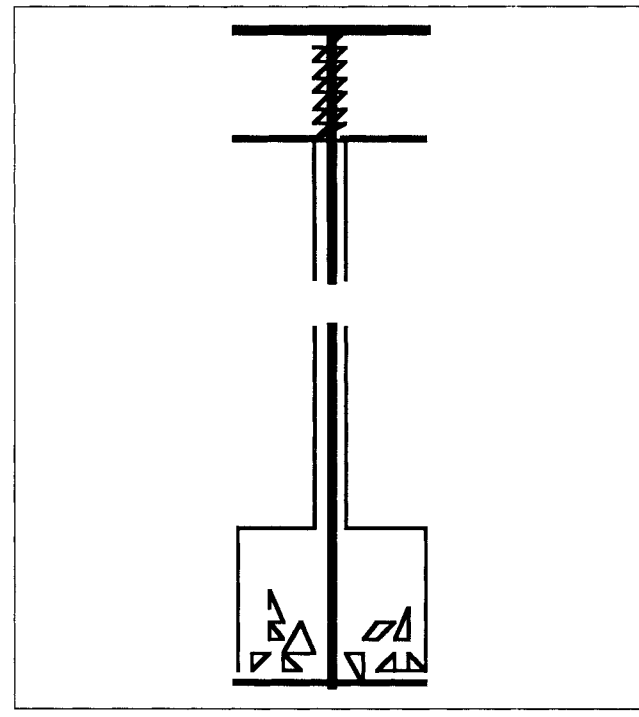

Figure 3. Device for introducing seed crystals.

Experimental Work

All the experiments have been performed in a 2.5-L controlled cooling crystallizer. The details of the crystallizer tank are given elsewhere (Qiu and Rasmuson, 1990). A flowsheet of the experimental apparatus is shown in Figure 2. The solid-liquid suspension in the vessel (1) is agitated by a propeller-type impeller driven by the motor (2). Any cooling curve can be activated by the computer (4), HP-86B. The computer outputs the temperature signal according to the cooling curve to the controller (5) as the set point. The PT 100 resistant thermometer (13) provides a measured value back to the controller. The controller operates on the three-way valve (10) to adjust the ratio of hot water (approximately 45°C) from the tank (7) to cold tap water from the tank (6) flowing through the crystallizer jacket. The data acquisition and control unit (3) measures the resistance of the PT 100 resistant thermometer (12), which is converted into temperature and stored in the computer. The accuracy of the temperature measurement is better than ±0.15°C. The pump (11) is used for the circulation of the cooling water. The heater (8) is used to maintain a higher temperature in the hot water tank; and (9) and (6) are overflow tanks.

The solution is prepared from recrystallized crystals of commercial succinic acid, initially with purity of 99.9 wt.%. The crystals are dissolved in distilled water. The solution is stirred for more than four hours at a temperature about 10°C higher than the initial temperature of the experiment. After the solution is charged into the crystallizer, a sample for determining the initial concentration is taken out. The starting temperature is approached by slow cooling. When the temperature reaches a stable value, a known amount of closely sized seed crystals is introduced to the crystallizer by the device shown in Figure 3, and the cooling program starts immediately. Using 10-mL glass pipettes, small samples of clear solution are withdrawn periodically (every 5 minutes) for concentration analysis. On the tip of the pipette, a cotton plug is fitted to prevent crystals from being sucked into the pipette. The concentration of the solution is determined using an Anton Paar DMA 60 density meter and the concentration vs. density relation (at 36.97°C) reported previously (Qiu and Rasmuson, 1990). The accuracy of the concentration measurement is better than ±0.1 g/kg water. The solubility of succinic acid in water has been measured previously (Qiu and Rasmuson, 1990). A second-order polynomial is used to correlate the solubility data. The temperatures are measured every 30 seconds. At the end of each experiment, the suspension is filtered and the product is dried for size analysis by sieving (DIN 4188).

A total of 12 different seeded, cooling crystallization experiments have been conducted and are presented in Table 1. The cooling curves follow:

$$\frac{T_0 - T}{T_0 - T_f} = \left(\frac{t}{t_f}\right)^x \tag{23}$$

and the value of the exponent, x, is given in the table.

Evaluation

The NAG library subroutine E02BAF is used to fit cubic splines to the experimental concentration and temperature vs. time data. The function value and its derivatives are evaluated by the subroutine E02BCF. Three equally-spaced (in time) interior knots are used in approximating the temperature vs. time curves. Two or three interior knots are used in approximating the concentration vs. time curves. The location of these are in general where the slope of the curve changes most pronouncedly. The cumulative undersize weight distribution of the product crystals mass

$$W(L_i) = \sum_{j=0}^{i-1} w_j \tag{24}$$

Table 1. Experimental Program*

Exp.	T_f °C	t_f min	x	N rpm	L_0 μm	M_0 g	Δc_0 g/kg	L_e μm	CV_e
E1	20	120	3	400	400–500	5.00	3.93	789	0.50
E2	20	120	2	400	400–500	2.22	3.64	755	0.48
E3	20	120	3	550	315–400	4.94	3.74	871	0.35
E4	20	120	2	550	250–315	4.54	6.09	985	0.30
E5	20	90	3	710	250–355	0.40	4.66	657	0.46
E6	20	90	2	710	250–355	0.30	3.96	594	0.46
E7	15	90	3	400	250–355	3.00	4.71	799	0.48
E8	15	90	2	400	250–355	0.30	6.14	541	0.40
E9	15	90	1.5	400	250–355	0.60	4.03	536	0.48
E10	20	90	2	400	250–355	0.50	3.84	521	0.45
E11	20	90	2	550	250–355	0.30	5.17	518	0.46
E12	20	90	1.5	710	250–355	0.30	3.84	567	0.45
Initial Temperature					30°C				
Amount of Solvent					2.5 kg				
Supersaturation Range					1–10 g/kg Water				
Final Magma Density					39–55 g/kg Water				
Seeded Crystals in the Product					10–70 wt.% (Very Approximate)				

*Dimensions for this table only.

is fitted by a spline with two or three interior knots. The interior knots are chosen in the same way as for the concentration data. The concentration vs. time function and the solubility curve calculated from the temperature function are plotted in Figure 4 for a typical experiment. The product crystal size distribution is plotted with the fitted spline in Figure 5 for this experiment.

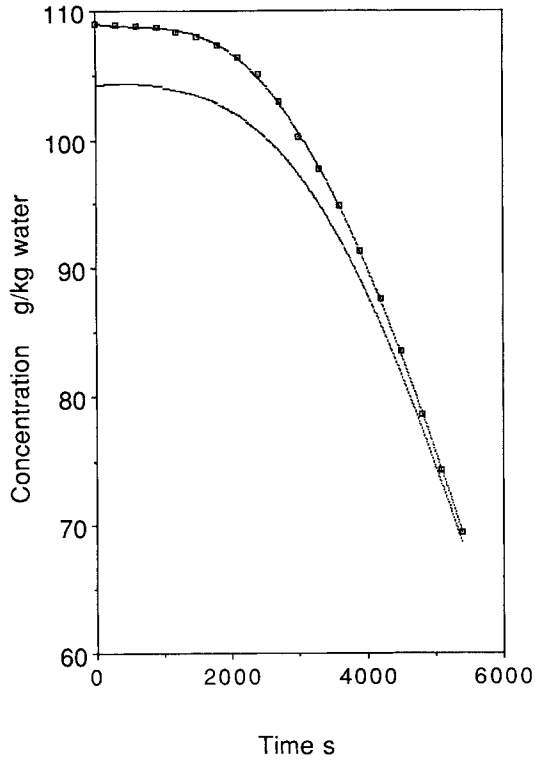

Figure 4. Experimental concentration vs. time data fitted with a spline (E5).

Lower curve shows corresponding solubility as obtained from temperature measurements.

The size of crystals remaining on the top sieve, 1,400 μm, is assumed to follow a constant slope of the $W(L)$ curve, and the maximum crystal size is calculated from the equation:

$$\int_{1,400}^{L_{max}} \left(\frac{dW}{dL}\right)_{L=1,400} dL = W(L_{max}) - W(1,400) \qquad (25)$$

in which $W(L_{max})$ is the sum of the crystal mass on all sieves.

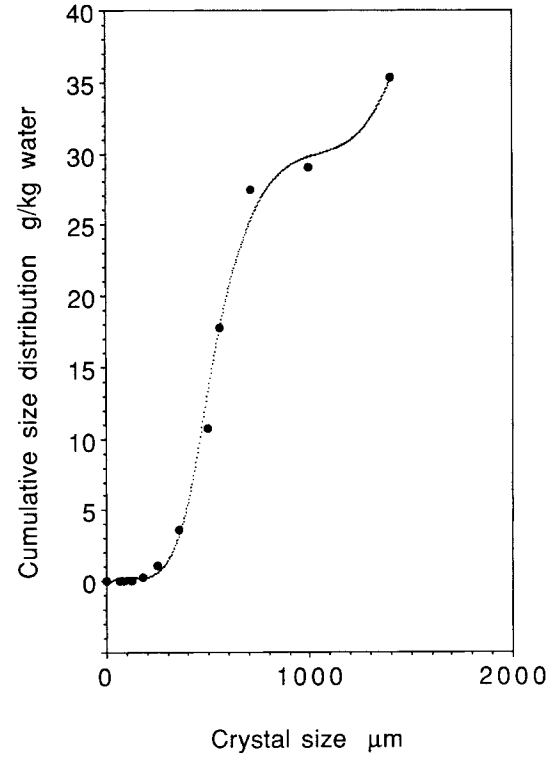

Figure 5. Cumulative product size distribution fitted with a spline (E5).

Thus, the correlated function always correctly describes the total mass. The mass of the crystals on the top sieve is usually rather low. The population density of the product crystals is calculated from the first derivative of the fitted spline:

$$n = \frac{1}{k_v \rho L^3} \frac{dW}{dL} \tag{26}$$

$k_v = 0.33$ was calculated from the shape information of Mullin and Whiting (1980) and is used in our calculation. During the period of starting the experiment and receiving the data on the product size distribution, some solute substance is lost due to sampling for concentration determination, in some cases for product size distribution determination by electrozone sensing technique, and in filtration and drying of the product. By a mass balance, the loss is found to range from 5 to 20 g (about 5 – 20% of the total product). An approximate correction for this loss has been done by multiplying the number of crystals of each fraction by a ratio of theoretical mass (using spline function concentrations):

$$W_f = W_0 + c_0 - c_f \tag{27}$$

and total mass on sieves:

$$W_F = k_v \rho \sum_{j=1}^{m} L_{0,j}^3 n_{0,j} \Delta L \tag{28}$$

that is,

$$\Delta N_j = n_{0,j} \Delta L \frac{W_f}{W_F} \quad (j = 1, 2, 3, \ldots, m) \tag{29}$$

Thus, the mass balance is fulfilled automatically in the calculations. Stepping terminates when the remaining mass equals or is less than the mass of seeds initially introduced. Ideally then, the total time in the calculations should equal the time of the experiment. In the calculations, the "remaining time" is of order 10 seconds or less, proving that the numerical procedure is adequate. In the calculations, a size interval of 4 μm is used for the discretization of the product population density distribution. A smaller size step does not influence the results significantly.

Usually, the concentration vs. time data and the final crystal size distribution can be fitted very well by the splines. The growth and the nucleation rates, however, are proportional to the first derivatives of these curves (Eqs. 13, 22 and 26) and are thus rather sensitive to scatter in data and quality of fit of approximating functions. When the amount of seeds is small, the concentration vs. time curve is very flat initially, and the relative error in the first derivative becomes significant. On the other hand, a larger amount of seeds will reduce the relative influence of nucleated crystals on the product size distribution, and nucleation data become more uncertain. The product size distribution of a seeded crystallizer is often bimodal, and it is not easy to approximate by a continuous function. Nucleation rates are calculated from a continuous function (a spline) fitted to the experimental product size distribution obtained by sieving. In particular, data corresponding to the size range "between" seeded crystals and nucleated crystals may be uncertain. These results originate from the initial part of the experiment and thus the final part of the calculations. Also, it may be assumed that the small size fraction of the product size distribution is less correctly measured and approximated. Accordingly, data of the early steps of the calculations should be handled more critically or even be excluded.

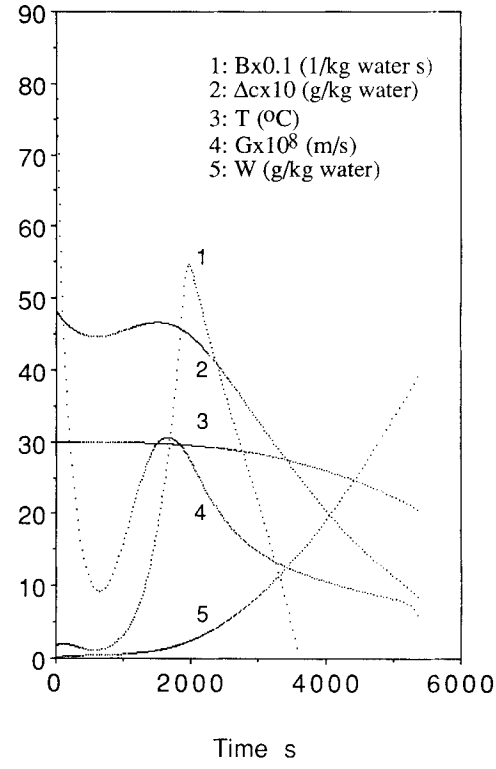

Figure 6. Output from the computer program (E5).

In Figure 6 the calculated crystal growth and nucleation rates, together with supersaturation, temperature and the magma density, are plotted against experiment time for the same experiment as in Figures 4 and 5. The very high growth rate early and even negative nucleation rate late (not shown) reveal the problems discussed previously. Otherwise, the results are very reasonable and what we would expect. Furthermore, there is a very good agreement between the maxima in the growth rate and the supersaturation curves. This is encouraging since the growth rate is calculated by Eq. 13 using concentration and size distribution data, while the supersaturation is calculated from concentration and temperature data. The maximum in the nucleation rate is also achieved where we expect to find it, that is, somewhat after the maximum in supersaturation, since the nucleation rate also depends on the magma density. Thus, we are rather confident that if the results are properly discriminated, adequate information may be obtained. About two thirds of the total range of data from each experiment are used for growth kinetics evaluation, and one third are used for the nucleation kinetics evaluation. Results from the early and late periods of each experiment are excluded.

The nucleation rates obtained from the experiments are extracted from the product crystal size distribution and accordingly represent an effective nucleation rate. Small crystals

growing very slowly are automatically excluded, especially because the results of the final part of each experiment are not used in evaluating kinetic parameters.

Results

The results are obtained as growth and nucleation rates at certain supersaturation values, temperatures and magma densities for each experiment. Using all adequate (above) results from the 12 different experiments simultaneously, kinetic parameters may be estimated. As a first approach, we assume size-independent growth. The crystal growth is usually considered to be a two-step process: diffusion of the solute from the bulk solution to the solution-crystal interface and the integration of the solute from the interface to the crystal lattice. It is often described by the expression:

$$\frac{G}{k_d}+\left(\frac{G}{k_r}\right)^{1/r}=\Delta c \tag{30}$$

However, if the growth rate data are correlated by this equation, the kinetic parameter values obtained are not realistic. In comparison to the results produced earlier (Qiu and Rasmuson, 1990), the present growth rate data are more scattered. In the present study, the conditions change considerably and the evaluation of growth rate data is more complicated in the presence of nucleation. The two-step model is sensitive to scatter, and problems of adopting Eq. 30 are discussed elsewhere (Qiu and Rasmuson, 1991). Furthermore, the volume diffusion resistance seems to dominate the growth process in the present experiments, and thus surface integration information is difficult to extract. By adopting a simple overall power law we may write:

$$G=k_g\Delta c^g N^p \tag{31}$$

During the experiments, the cooling rate is controlled to keep the supersaturation within the metastable range, and accordingly secondary nucleation dominates (in comparison to primary nucleation). Contact secondary nucleation is regarded as the most important source of secondary nucleation in a crystallizer and is usually described by a power law expression (Garside, 1985):

$$B=k_B\Delta c^b M_T N^h \tag{32}$$

Even though a first-order dependence on the magma density is usually assumed, nonunity exponents are sometimes reported. However, from the experimental data we are not able to obtain reliable values on four nucleation parameters. Equations 31 and 32 are applied to correlate the data from all 12 experiments using the NAG subroutine E04FCF. The parameters are given in Table 2. The output data of this subroutine allow for computation of the inverse of the Hessian as $0.5(VS^{-1})(VS^{-1})^T$. Confidence ranges are estimated as suggested in the introduction to E04 routines of NAG. We do not account for that data are interrelated within each experiment. The goodness of fit for nucleation and growth are shown in Figures 7 and 8, comprising all data included in the optimizations. The points of each experiment line up in the diagrams,

Table 2. Kinetic Parameters Assuming Size-Independent Growth*

k_g	$(1.04\pm0.06)\times10^{-6}$
g	1.05 ± 0.03
p	0.63 ± 0.06
k_B	$(5.61\pm2.20)\times10^{7}$
b	4.01 ± 0.20
h	2.28 ± 0.16

* ±95% confidence limits.

showing that residuals within each experiment are not normally distributed. This is not unexpected since data within each experiment are interrelated from a physical point of view as well as by the evaluation procedure. Concentration and size measurements are approximated by functions that result in smoothing of experimental scatter. It is not surprising that there is the wide range of residuals, since only three constants for growth and nucleation are used to describe data points from 12 significantly different experiments.

In the experiments, the temperature range is narrow and becomes even more reduced by discriminating initial and final periods of each experiment as discussed before. A correlation including an overall activation energy for the crystal growth rate does not improve the goodness of fit significantly. In a previous article (Qiu and Rasmuson, 1990), size-dependent growth was observed and accounted for in a two-step expression and in an equation of overall power law type. Unfortunately, none of these equations may be applied here since the two-step equation does not fulfil the assumption of Eq. 4, and the power law equation results in zero growth rate at zero size. The previous experimental results (Qiu and Rasmuson, 1990),

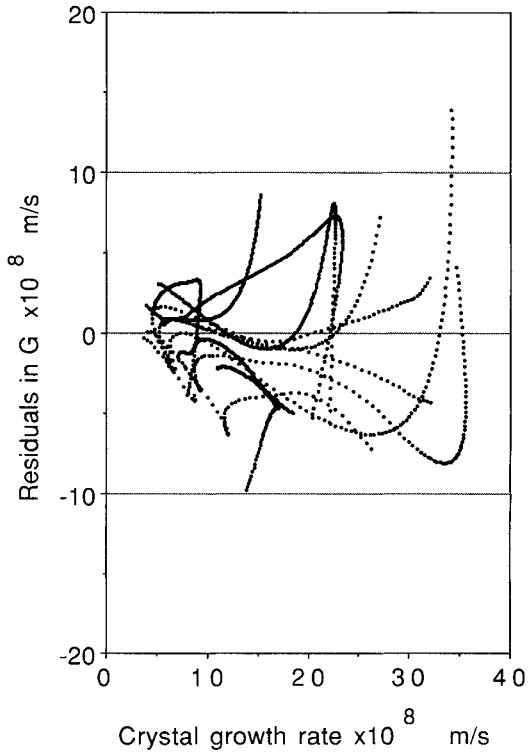

Figure 7. Goodness of fit of the crystal growth rates by Eq. 31.

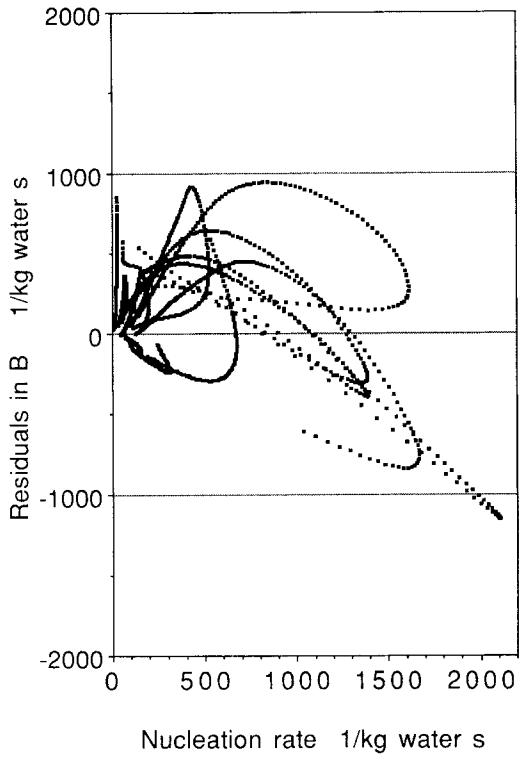

Figure 8. Goodness of fit of the nucleation rates by Eq. 32.

however, may be approximated by an overall power law equation comprising a linear (Canning and Randolph, 1967) size-dependency. (A nonunity exponent on the parenthesis could not be successfully extracted.)

$$g(L) = (1 + 1.477 \times 10^3 L) \tag{33}$$

Equation 33 predicts about a factor of two change in growth rate with size over the size range of the present experiments. Using Eq. 33, the growth rate function $f(\Delta c)$ and nucleation rate can be evaluated by the procedure described. A power law equation can then be used to correlate the values of $f(\Delta c)$ as:

$$f(\Delta c) = k_g \Delta c^g N^p \tag{34}$$

The growth and nucleation parameters obtained are shown in Table 3. The crystal growth rate parameters (g and p) in Table 3 agree very well with the parameters in Table 2. The nucleation rate parameters (b and h) in Tables 2 and 3 do agree reasonably well. The growth rate is likely to be dominated by volume diffusion, and thus it may be more appropriate to include the corresponding inverse dependence on size (Levins and Glastonbury, 1972). In this case, however, we obtain nucleation parameter values that are less realistic.

Table 3. Kinetic Parameters Assuming Size-Dependent Growth*

k_g	$(8.29 \pm 0.45) \times 10^-$
g	1.09 ± 0.03
p	0.63 ± 0.06
k_B	$(3.35 \pm 4.58) \times 10^6$
b	4.22 ± 0.67
h	2.88 ± 0.48

* ±95% confidence limits.

Discussion

Kinetics

Previously published results (Mullin and Whiting, 1980; Qiu and Rasmuson, 1990) reveal a growth rate order with respect to supersaturation of approximately 1.8. The value found in the present work is significantly lower, close to unity. The order with respect to impeller speed in the present study is 0.63, which is higher than the earlier result of 0.36 (Qiu and Rasmuson, 1990). Actually, the values of these parameters suggest that on average the volume diffusion step is dominant in the present experiments. At pure volume diffusion control we expect the growth rate to be directly proportional to supersaturation, and the volume diffusion mass transfer constant depends on stirring rate to order about 0.62 (Levins and Glastonbury, 1972).

According to previous results (Qiu and Rasmuson, 1990), larger crystals and higher supersaturation decrease the surface integration effectiveness factor, thus the volume diffusion resistance becomes more dominant. In the present experiment, supersaturation during certain periods increases significantly above 5 g/kg water. Also, the size range is extended far above 755 μm (as being the largest mean size in the previous work). However, product mean sizes range from about 500 to 900 μm, and time averaged mean sizes are, of course, even lower. Thus, the size is on average within the range of the previous work. The low growth rate order may, however, also relate somewhat to shape effects. A significant fraction of larger crystals in the product are rounded as a result of attrition. Also, a decrease in the relative thickness is observed in the product crystals as compared to the seed crystals. If there is a gradual area increase during the experiments, not included in the size or number increase, a lower growth rate order may result from the calculations.

No previous results on nucleation rates of succinic acid have been found. Dependence on supersaturation to the power 4 is somewhat higher than expected for secondary nucleation in general (Garside and Davey, 1980). Dependence on the stirring rate, to the power 2.3, observed in this study is a bit lower than expected. Theoretical discussions suggest a range of 3–4 (Garside and Davey, 1980), but lower values are sometimes found in practice (Garside and Shah, 1980). Low values on the order of the stirring rate dependence may reflect regeneration or survival-limited nucleation (Garside and Shah, 1980). On the other hand, recent derivations by Pohlisch and Mersmann (1988) suggest an exponent of 2.2, when fragmentation is important.

In Figure 9 we compare growth rates obtained in the present work with earlier results. The experiments in this study are performed in the same crystallizer as used previously (Qiu and Rasmuson, 1990), and the comparison is made for the impeller speed (in Eq. 31 and the previous two-step equation) of 221 rpm, at which the volume diffusion mass transfer constant equals the value of Mullin and Whiting (1980), 4.59×10^{-5} m/s. The experiments of Mullin and Whiting were performed at 27.3°C, and thus this is also the temperature used in the pre-

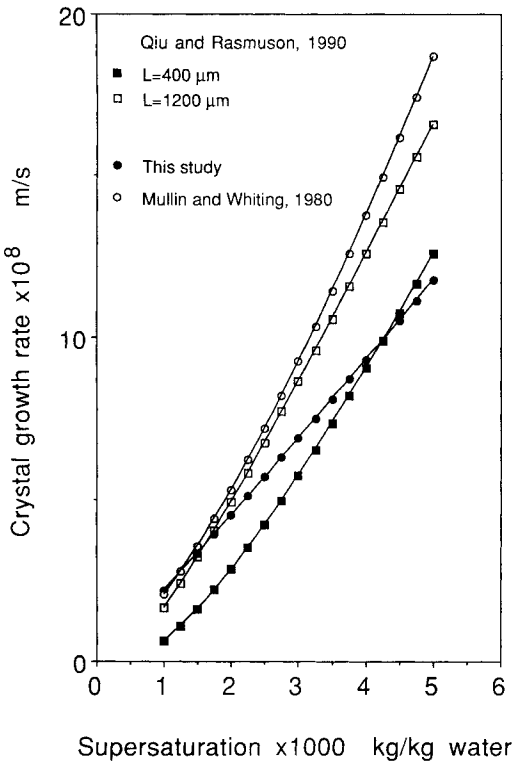

Figure 9. Growth rates: this study vs. previously published data.

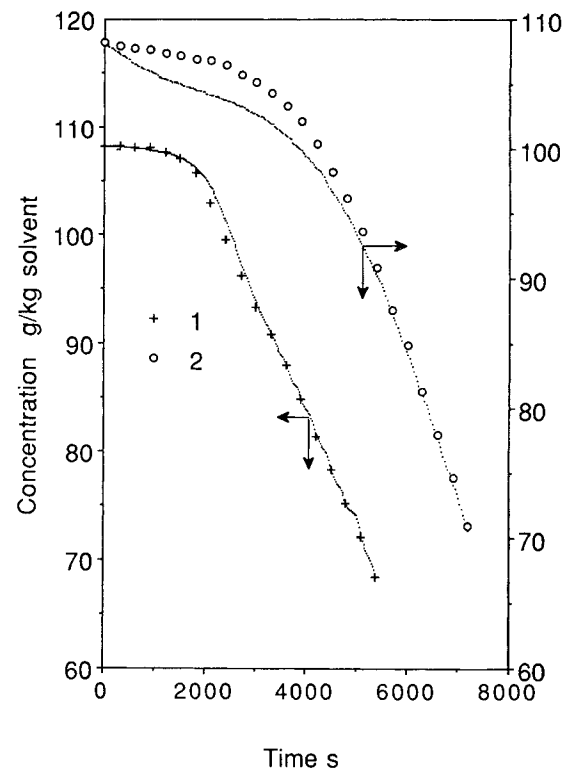

Figure 10. Measured and predicted concentration vs. time data.

Curve 1, nucleated crystals dominate (E5); curve 2, seeded crystals dominate (E3).

vious two-step relation. The crystal growth rates in the present study are in very good agreement with previously published data.

Computer simulation of cooling crystallization

Using the kinetic parameters of Table 2, we may computer-simulate the cooling crystallization experiments. The method of characteristics is used to solve the population balance equation, Eq. 1. Input to the simulations are temperature profile, seed amount and size, total time, initial concentration, kinetics and solubility data. Output results are the concentration vs. time curve and the final crystal size distribution. Comparisons of experimental and predicted results are presented in Figures 10 and 11. The experimental product size distributions are given as cumulative mass below each sieve. The shape of the distribution curves clearly exposes a product comprising seeded and nucleated crystals. When nucleated crystals dominate the product (case 1), the concentration curve and product size distribution are predicted well. When seeded crystals dominate the product (case 2), discrepancies between predictions and experimental data may be observed. The concentration, during the early part, is underestimated, and the weight fraction of seeded crystals in the product is overestimated.

In Figures 12 and 13 we compare predicted and experimentally-obtained weight mean sizes and coefficients of variations (*CV*) of the product. The experimental weight mean sizes cover a range from 0.5 to 1 mm as a result of the wide range of conditions in the experimental program. With one exception, the predicted weight mean sizes are within 25% of the experimental results, but they tend to be overestimated. In calcu-

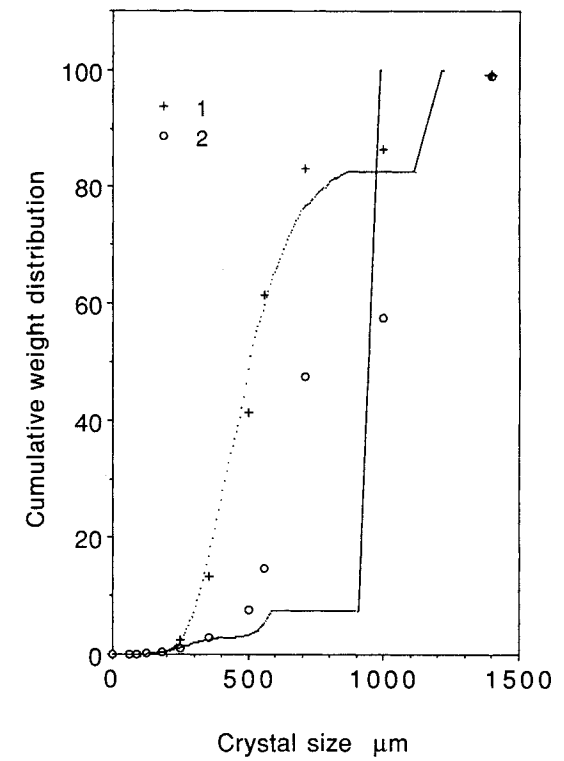

Figure 11. Measured vs. predicted crystal size distributions.

Curve 1, nucleated crystals dominate (E5); curve 2, seeded crystals dominate (E3).

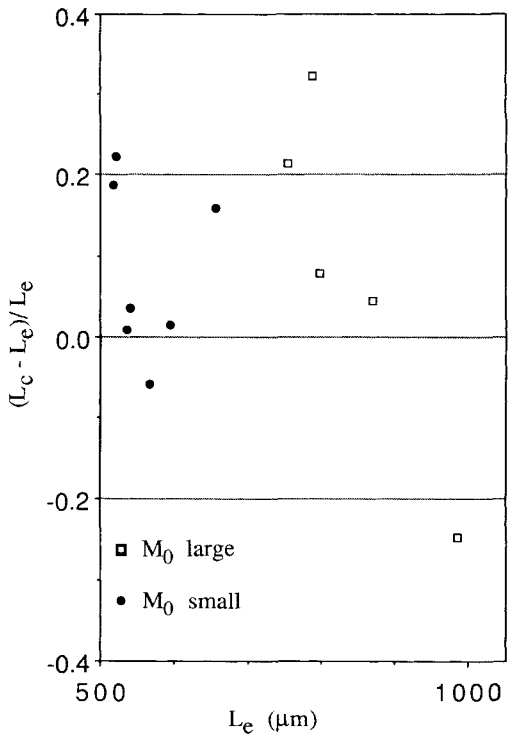

Figure 12. Predicted vs. experimental mean sizes.

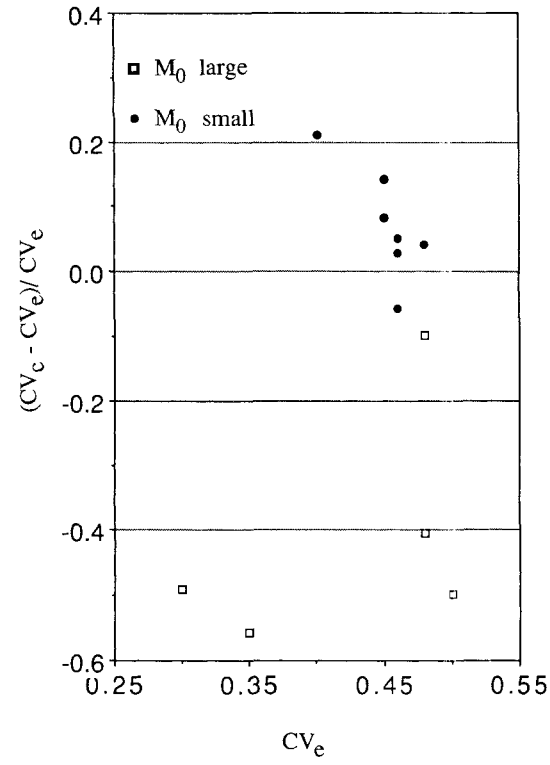

Figure 13. Predicted vs. experimental coefficients of variation.

lating the experimental mean size and *CV* of the product, the total mass of a sieve fraction is allocated to a size equal to the arithmetic mean of the upper and lower sieve. Even though the mass of nucleated crystals in the product may be assumed to be a rather monotonous function of size, it is not necessarily true for seeded crystals. The upper part of the cumulative mass distribution curve is likely to be more or less S-shaped as it originates from a narrow fraction of seeds. Furthermore, the number of sieves in the upper range is very limited and the size range of each sieve fraction is wide. Thus, the experimental mean size and *CV* values do contain uncertainties, which increases with increasing mass fraction of seeded crystals in the product, and we regard the prediction of the mean sizes to be rather good. Coefficients of variations are predicted well for experiments with a small amount of seeds. For the experiments with a large amount of seeds, predicted values are, with one exception, always significantly lower than the experimental ones. The coefficient of variation is influenced strongly by the bimodal character of the product and thus by the mass ratio of seeded to nucleated crystals in the product. In cases of large amounts of seeds, the mass fraction of seeded crystals is overestimated significantly; occasionally values up to 90% are predicted when experimental values are approximately 50%.

In the results presented, systematic discrepancies can be observed, indicating that some features of the kinetics are not accounted for. For all experiments, there is a systematic overestimation of the product mass related to seeds, and occasionally there is at least a slight underestimation of their final size. These effects can be explained by a decreasing shape factor which corresponds to the observation that large, seeded crystals in the product are more window-like. Since the predictions assume a constant volume shape factor, a certain size increase is calculated to consume more supersaturation and deposit more mass than is true in reality. The first effect reduces the supersaturation and thus lowers the extent of growth for both seeds and nucleated crystals, and the second effect overestimates the mass of seeded crystals in the product. Unfortunately, a shape parameter cannot be extracted by regression on the information at hand, but demands further experimental characterization of the product.

It is possible, but with decreased confidence, to extract four nucleation parameters including an exponent on the magma density. Assuming growth to be size-independent, the magma density exponent becomes 0.35, the exponent on supersaturation 2.5 and on stirring rate 1.1. Using these kinetics, the mass fraction of seeded to nucleated crystals in the product is better described and the normalized residuals of mean size and *CV* (Figures 12 and 13) scatter closer to zero. However, there are still systematic discrepancies, and predictions of concentration curves are less accurate. Growth rate dispersion is a possibility. However, since the size distribution data are very sparse and the product distribution of seeded crystals tends to be S-shaped, we find no clear evidence of significant growth dispersion. Also, the kinetic constants obtained suggest that volume diffusion is essentially controlling.

Method

The method proposed here resembles a method proposed earlier (Nyvlt, 1989), in that the same experimental information is exploited. However, by performing the back shift of the size distribution by defining a size step, instead of a time step, calculations become explicit, instead of implicit. In comparison to the methods where the size distribution is measured several times during the experiment (Misra and White, 1971; Tavare and Garside, 1986), the method presented has the advantage that deficiencies in representation of the size distribution in

the small size region become relatively unimportant. On the other hand, a limited resolution in characterizing large crystals is a problem. In particular, the product size of seeded crystals becomes uncertain and thus the appropriate mass change in the stepping procedure. This problem is reduced by including several different experiments simultaneously into the determination of kinetics and by reducing the mass fraction of seeded crystals in the product. However, if we exclude the five experiments in which the seeded crystals almost dominate the product, values of kinetic constants do not change considerably (apart from p that increases to unity), residual diagrams are in principle unaltered and the predictions of mean size and CV are essentially the same (for the seven remaining experiments). An unattractive step in the method is the approximation of concentration and size distribution data by functions, which are then used for evaluation of derivatives. However, in the present work, kinetics can be extracted that are physically reasonable, correspond well with previous results, and do predict batch cooling crystallization experiments rather well.

Conclusions

A method to evaluate crystal growth rates and nucleation rates simultaneously from batch cooling experiments is presented. The population balance equation is solved numerically by the method of characteristics. Concentration and temperature are recorded during the experiments, and the final crystal size distribution is analyzed. In comparison to the traditional MSMPR technique, the proposed method is significantly more efficient. Also, nucleation rates are related directly to the product crystals, instead of relying on uncertain extrapolations to zero size. In comparison to batch techniques based on recording the evolution of the size distribution, the present method has the advantage of being less sensitive to the accuracy in determination of the small-size fraction. Using the method proposed, nucleation and growth rates for succinic acid are determined. Growth rates are in good agreement with results previously published. Using the kinetic parameters determined, cooling crystallizations may be simulated producing reasonably accurate predictions of product size distributions.

Acknowledgment

The financial support of The Swedish Board for Technical Development (STU), The Swedish Council for Planning and Coordination of Research (FRN), and The Swedish Industrial Association for Crystallization Research and Development (IKF) are gratefully acknowledged.

Notation

b = nucleation order
B = nucleation rate, 1/s kg solvent
c = concentration, kg/kg solvent
c^* = solubility, kg/kg solvent
c_i = interfacial concentration, kg/kg solvent
CV_c = predicted product coefficient of variation
CV_e = experimental product coefficient of variation
Δc = supersaturation, kg/kg solvent
f = time dependent part of the growth rate, m/s
G = crystal growth rate, m/s
g = size-dependent part of the growth rate, order for power law equation
h = nucleation order with respect to N
J = Jacobian matrix
k_B = nucleation rate coefficient
k_d = mass transfer coefficient for crystal growth, m/s kg solvent/kg crystal
k_g = coefficient for power law equation
k_r = surface integration constant
k_v = volumetric shape factor
L = crystal size, m
L_c = predicted product weight mean size, m
L_e = experimental product weight mean size, m
$L_{i,j}$ = mean size of jth group of crystals after ith step calculation, m
M_T = total crystal mass, kg/kg solvent
M_0 = mass of seeds added, kg
m = number of the discretization of the product size
N = impeller speed, rpm
ΔN = number of crystals, no./kg solvent
ΔN_j = number of jth group of crystals, no./kg solvent
n = population density, 1/m kg solvent
n_0 = population density of seeds, 1/m kg solvent
$n_{0,j}$ = product population density of jth group of crystals, 1/m·kg solvent
p = growth order with respect to N
r = order of surface integration
S = vector of singular values of the estimated Jacobian matrix
T = temperature, °C
t = time, s
V = matrix of orthonormalized eigenvectors of J^TJ
W = cumulative mass of crystals, kg/kg solvent
W_F = the mass of the product crystals, kg/kg solvent
w_j = mass of crystals on jth sieve
x = exponent for the temperature profile

Greek letters

Δ = difference
ρ = density of crystalline material, kg/m^3
θ = time, s

Subscripts

0 = initial
f = final

Literature Cited

Baliga, J. B., "Crystal Nucleation and Growth Kinetics in Batch Evaporative Crystallization," PhD Thesis, Iowa State Univ., Ames, IA (1970).

Bransom, S. H., and W. J. Dunning, *Kinetics of Crystallization: II*, Discussions, Faraday Society, No. 5, 96 (1949).

Bujac, P. D. B., and J. W. Mullin, "A Rapid Method for the Measurement of Crystal Growth Rates in a Fluidized Bed Crystallizer," *Symp. Ind. Crystall.*, The Institution of Chemical Engineers, London, 121 (Apr., 1969).

Canning, T. F., and A. D. Randolph, "Some Aspects of Crystallization Theory: Systems that Violate McCabe's Delta L Law," *AIChE J.*, **13**(1), 5 (1967).

Davey, R. J., J. W. Mullin, and M. J. L. Whiting, "Habit Modification of Succinic Acid Crystals Grown from Different Solvents," *J. Crystal Growth*, **58**, 304 (1982).

Garside, J., "Industrial Crystallization from Solution," *Chem. Eng. Sci.*, **40**, 3 (1985).

Garside, J., and R. J. Davey, "Secondary Contact Nucleation: Kinetics, Growth and Scale-Up," *Chem. Eng. Commun.*, 393 (1980).

Garside, J., and M. B. Shah, "Crystallization Kinetics from MSMPR Crystallizers," *Ind. Eng. Chem. Process Des. Dev.*, **19**, 509 (1980).

John, F., *Partial Differential Equations*, 3rd ed., Springer-Verlag, New York (1978).

Levins, D. M., and J. R. Glastonbury, "Particle-Liquid Hydrodynamics and Mass Transfer in a Stirred Vessel," *Trans. Instn. Chem. Engrs.*, **50**, 132 (1972).

Marchal, P., R. David, J. P. Klein, and J. Villermaux, "Kinetics of Adipic Acid Crystallization in a Semi-batch Crystallizer," *New Ap-*

proaches to Batch Crystallization, IChemE/BACG Joint Meeting (Sept. 27, 1988).
Mullin, J. W., and M. J. L. Whiting, "Succinic Acid Crystal Growth Rates in Aqueous Solution," *Ind. Eng. Chem. Fund.*, **19**, 117 (1980).
Misra, C., and E. T. White, "Kinetics of Crystallization of Aluminum Trihydroxide from Seeded Caustic Aluminate Solutions," *AIChE Symp. Ser.*, **67**(110), 53 (1971).
Ness, J. N., and E. T. White, "Collision Nucleation in an Agitated Crystallizer," *AIChE Symp. Ser.*, **72**(153), 64 (1976).
Nyvlt, J., "Calculation of the Kinetics of Crystallization Based on a Single Batch Experiment," *Collect. Czech. Chem. Commun.*, **54**, 3187 (1989).
Omran, A. M., and C. J. King, "Kinetics of Ice Crystallization in Sugar Solutions and Fruit Juices," *AIChE J.*, **20**(4), 795 (1974).
Pohlisch, J. R., and A. Mersmann, "The Influence of Stress and Attrition on Crystal Size Distribution," *Chem. Eng. Technol.*, **11**, 40 (1988).
Qiu, Y., and Å. C. Rasmuson, "Evaluation of Kinetic Data from Batch Experiments," *Industrial Crystallization 87*, J. Nyvlt and S. Zacek, eds., Elsevier, Amsterdam, p. 329 (1989).
Qiu, Y., and Å. C. Rasmuson, "Growth and Dissolution of Succinic Acid Crystals in a Batch Stirred Crystallizer," *AIChE J.*, **36**(5), 665 (1990).
Qiu, Y., and Å. C. Rasmuson, "Crystal Growth Rate Parameters from Isothermal Desupersaturation Experiments," *Chem. Eng. Sci.*, **46**(7), 1659 (1991).
Randolph, A. D., and M. A. Larson, *Theory of Particulate Technology*, Academic Press, New York (1971).
Tanimoto, A., K. Kobayashi, and S. Fujita, "Overall Crystallization Rate of Copper Sulfate Pentahydrate in an Agitated Vessel," *Int. Chem. Eng.*, **4**(1), 153 (1964).
Tavare, N. S., and J. Garside, "Simultaneous Estimation of Crystal Nucleation and Growth Kinetics from Batch Experiments," *Chem. Eng. Res. Des.*, **64**, 109 (1986).
Verigin, A. N., I. A. Shchuplyak, M. F. Mikhalev, and V. N. Kulikov, "Investigation of Crystallization Kinetics with Programmed Variation of the Solution Temperature," *Zhurnal Prikladnoi Khimii*, **52**(8), 1898 (1979).
Witkowski, W. R., S. M. Miller, and J. B. Rawling, "Light-Scattering Measurements to Estimate Kinetic Parameters of Crystallization," *Crystallization As a Separation Process, ACS Symp. Ser.*, No. 438, 102, A. S. Myerson and K. Toyokura, eds., Washington, DC (1990).

Manuscript received Dec. 28, 1990, and revision received June 13, 1991.